FORMULATION OF THE ECMWF MODEL

M. Hortal
European Centre for Medium-Range Weather Forecasts
Shinfield Park, Reading, U.K.

1. INTRODUCTION

During the last couple of years, a major reformulation of the dynamics of the ECMWF model has taken place in order to increase its efficiency. With these changes and the new CRAY YMP installed in June 1990, the model resolution has been increased to T213 and 31 levels. An indication of the benefit likely to be obtained with the new horizontal resolution can be seen from the representation of the orography which is shown over Europe in Fig. 1 if we compare it with the corresponding representation from the T106 model.

The two main changes have been the treatment of advection by means of the semi-Lagrangian technique (cf *Robert*, 1982) and the introduction of the "reduced Gaussian grid" (cf *Hortal & Simmons*, 1991). Consistent with these changes, the I/O between the model and secondary storage has also undergone a complete revision and the calculation of the Legendre transforms has been made more efficient.

The model uses the spectral representation in the horizontal based on spherical harmonics and therefore only scalar fields can be treated in this space. Accordingly, the spectral representation of the momentum quantities is in the usual form of vorticity and divergence from which the components of the horizontal wind are computed. As the divergence equation previously used does not have a proper advective form which allows the semi-Lagrangian treatment, the form of the momentum equations treated in grid-point space is the wind components form (u-v formulation).

In the vertical, a hybrid coordinate is used, as in the previous operational model, which changes gradually from the terrain-following sigma coordinate at the lowest levels to a pressure coordinate at the uppermost levels. The new distribution of levels is sketched, together with the old one in Fig. 2.

2. MODEL EQUATIONS

Momentum:

$$\frac{d\,\vec{V}_h}{d\,t} = -\nabla_\eta \Phi - R_d\,T_V\,\nabla_\eta \ln p - f\,\vec{k}\,X\,\vec{V}_h + P_{\vec{V}_h} + K_{\vec{V}_h} \qquad (2.1)$$

here ∇_η is the gradient along a constant vertical coordinate plane and V_h is the "horizontal" wind on the same plane.

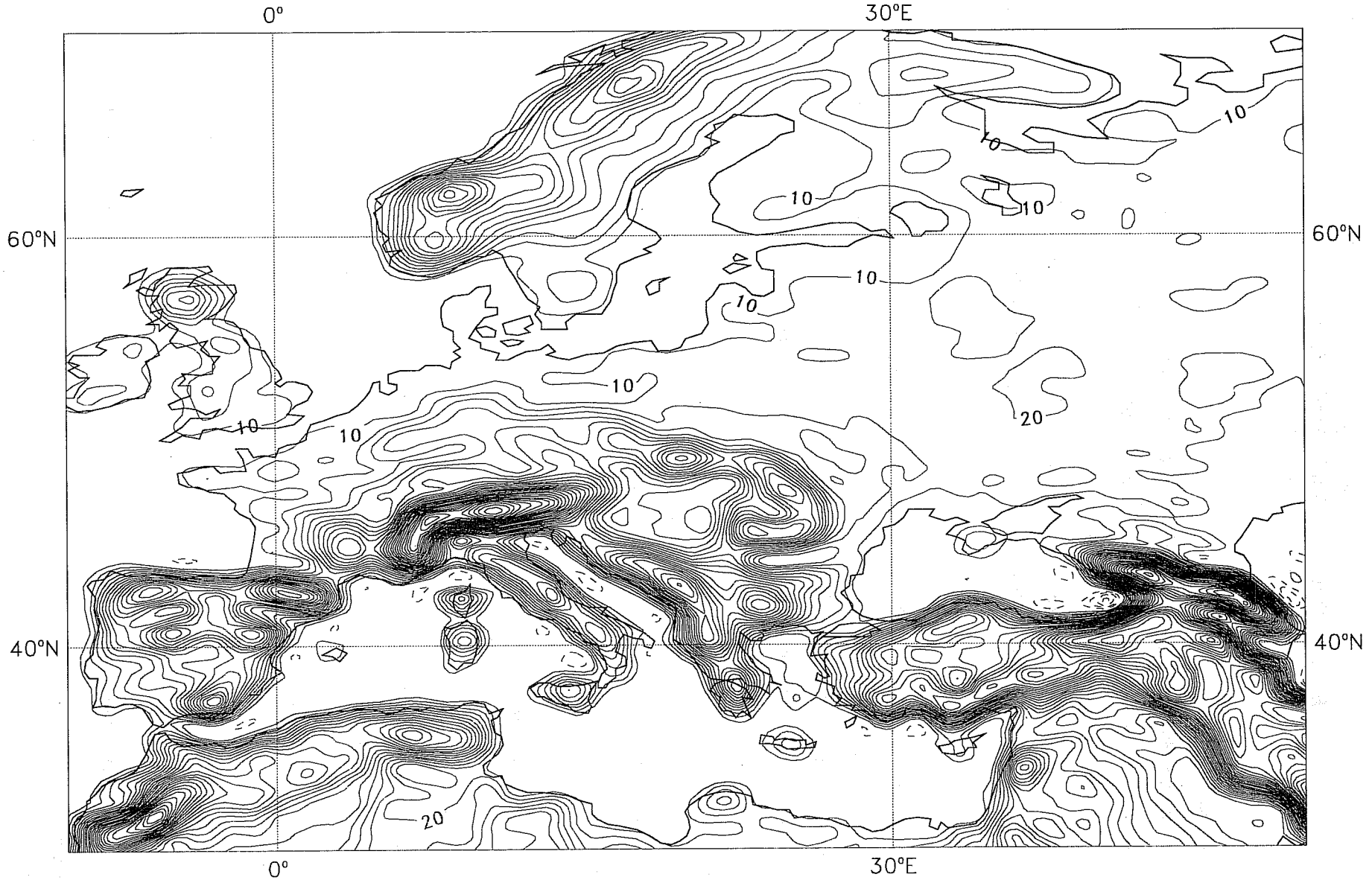

Fig. 1 Orography of Europe in the new T213 model (dam)

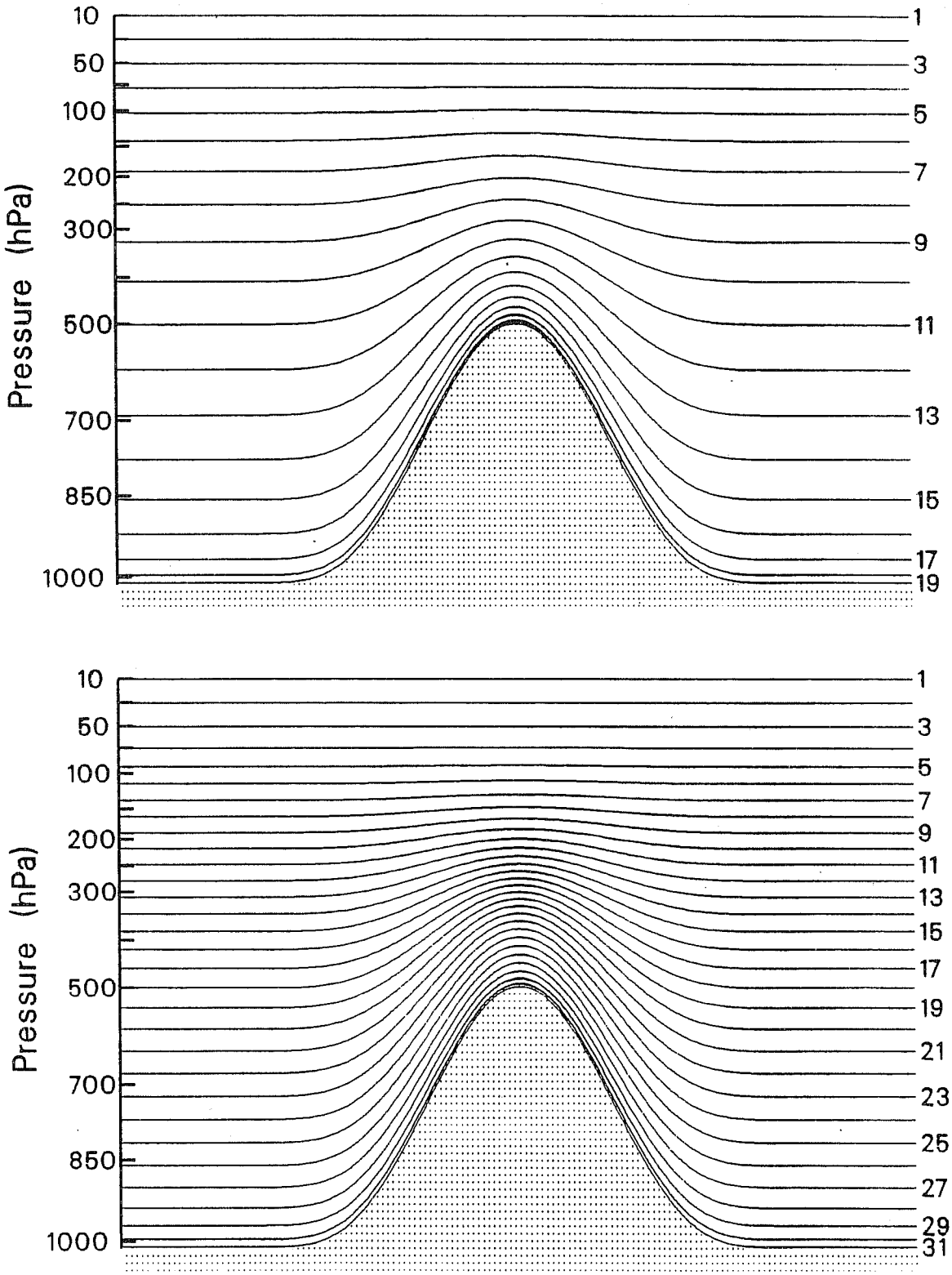

Fig. 2 Schematic representation of the position of the hybrid vertical levels in the old (19 levels) and in the new (31 levels) models.

Thermodynamic:

$$\frac{d\,T}{d\,t} = \frac{K\,T_V}{[1 + (\delta - 1)\,q]}\frac{\omega}{p} + P_T + K_T \tag{2.2}$$

Moisture:

$$\frac{d\,q}{d\,t} = P_q \tag{2.3}$$

Continuity:

$$\frac{d}{d\,t}\left(\frac{\partial p}{\partial \eta}\right) = -\frac{\partial p}{\partial \eta}\left(D + \frac{\partial \dot{\eta}}{\partial \eta}\right) \tag{2.4}$$

Hydrostatic:

$$\frac{\partial \phi}{\partial \eta} = -\frac{R_d\,T_V}{p}\frac{\partial p}{\partial \eta} \tag{2.5}$$

Integrating the continuity equation with $\dot{\eta}=0$ for $\eta=0$ and $\eta=1$ we get:

$$\dot{\eta}\frac{\partial p}{\partial \eta} = -\frac{\partial p}{\partial t} - \int_0^{\eta} \nabla \cdot \left(\vec{V}_h \frac{\partial p}{\partial \eta}\right) d\,\eta \tag{2.6}$$

and

$$\frac{\partial\, p_s}{\partial\, t} = -\int_0^1 \nabla \cdot \left(\vec{V}_h \frac{\partial\, p}{\partial\, \eta}\right) d\eta \tag{2.7}$$

or, using $p = A + B\,p_s$, the pressure on a hybrid plane defined by the parameters A and B:

$$\dot{\eta}\left(\frac{\partial\, p}{\partial\, \eta}\right) = B(\eta)\int_0^1 \nabla \cdot \left(\vec{V}_h \frac{\partial\, p}{\partial\, \eta}\right) d\eta - \int_0^{\eta} \nabla \cdot \left(\vec{V}_h \frac{\partial\, p}{\partial\, \eta}\right) d\eta \tag{2.8}$$

$$\frac{\partial B}{\partial \eta}\frac{d \ln p_s}{d\,t} = -\frac{1}{p_s}\left[\frac{\partial B}{\partial \eta}\int_0^1 \nabla\left(\vec{V}\frac{\partial p}{\partial \eta}\right)d\eta + \vec{V}\cdot\nabla\frac{\partial p}{\partial \eta}\right] \tag{2.9}$$

Here:

$$\frac{dA}{dt} = \frac{\partial A}{\partial t} + \vec{V}_h \cdot \nabla_\eta A + \dot{\eta} \frac{\partial A}{\partial \eta} \tag{2.10}$$

is the Lagrangian time derivative.

The P terms on the right hand side are the parametrized physical tendencies and the K's are the "horizontal" diffusion terms.

3. SEMI-LAGRANGIAN PROCEDURE

Let

$$\frac{dA}{dt} = 0 \tag{3.1}$$

then the quantity A of an air parcel is conserved in a reference system which moves with the parcel.

- Lagrangian procedure: Starting from a regular grid of points, the trajectory of the air parcel surrounding each of them is computed and the value of field A at the end point, after one time-step is set equal to its value at the starting point and time. The problem is that the resulting set of points no longer form a regular array and therefore are not easy to handle.

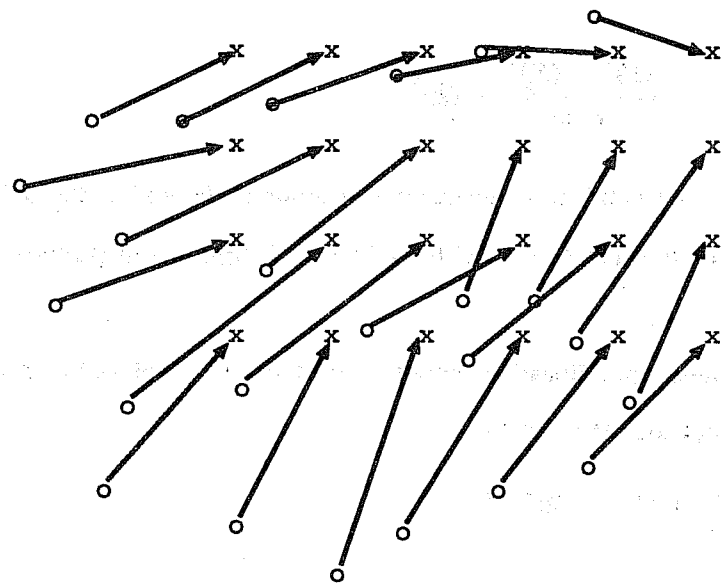

Fig. 3 Schematic of the semi-Lagrangian procedure. The arrival points (x) form a "regular" grid while the departure points (o) are irregularly placed.

- Semi-Lagrangian procedure: In this approach, the arrival points are taken to form a regular grid. The trajectory of the parcels arriving at them is traced back and the value of field A at these starting points is calculated by means of interpolation.

- Non-interpolating semi-Lagrangian procedure: Once the trajectory of the parcels has been traced back, the semi-Lagrangian discretization is applied from the grid point nearest to the departure point, the rest of the advection of the field being treated in an Eulerian way.

4. DISCRETIZATION

The representation of the horizontal fields is spectral, with triangular truncation at 213 wavenumbers chosen for the operational resolution. As usual, the non-linear terms and the parametrizations are calculated over a Gaussian grid to be described later on. The humidity is kept in the Gaussian representation when the option of shape-preserving interpolation is used for the semi-Lagrangian treatment of its advection.

The vertical discretization uses a hybrid coordinate η which becomes a σ coordinate near the surface and a pressure coordinate near the top with a smooth transition in between (cf *Simmons & Burridge*, 1981; *Simmons & Strüfing*, 1981).

The semi-Lagrangian discretization is an adaptation of Ritchie's approach (cf *Ritchie*, 1987 & 1988) within the framework of the hybrid vertical coordinate system. The total time derivatives are approximated as follows:

$$\frac{dF}{dt} = R \quad \Rightarrow \quad \frac{(F)^{+} - (F_f)^{-}}{2\,\Delta t} = (R)^{0} \tag{4.1}$$

where $()^{+}$, $()^{-}$ and $()^{0}$ correspond to the evaluation of terms at the end of the trajectory (time $t+\Delta t$), the beginning of the trajectory (time $t-\Delta t$) and the middle of it (time t) respectively.

The semi-implicit treatment of a linearized gravity-wave term $\bar{X}$ is achieved by adding to the explicit r.h.s. of the corresponding equation the quantity

$$\bar{X} \rightarrow \frac{\beta}{2}\,[(\bar{X})^{+} + (\bar{X}_f)^{-} - 2(\bar{X})^{0}] \tag{4.2}$$

this is computed as

$$\bar{X} = \frac{\beta}{2}\,[\bar{X}^{+}(t+\Delta t) + \bar{X}_f^{-}(t-\Delta t) - \bar{X}^{+}(t) - \bar{X}^{-}(t)] \tag{4.3}$$

Currently, $\beta = 1$.

In the momentum equation, the linearized term:

$$- \nabla_\eta (\bar{\phi} + R_d T_r \ln p_s) \tag{4.4}$$

is treated semi-implicitly where

$$\bar{\phi} = \phi_s - R_d \int_1^\eta T \frac{d}{d\eta}(\ln \bar{p})\, d\eta = \phi_s + \gamma T \tag{4.5}$$

and $\bar{p}$ is the pressure corresponding to a constant surface pressure p_r of 800 hPa.

In the thermodynamic equation, the term

$$K T_r \left(\frac{\dot{\omega}}{p}\right) = -\frac{K T_r}{\bar{p}} \int_0^\eta D \frac{d\bar{p}}{d\eta}\, d\eta = -\tau D \tag{4.6}$$

is treated semi-implicitly.

Here T_r is a constant reference temperature of 300 K.

In the continuity equation, the term

$$- \frac{d\bar{p}}{d\eta} D \tag{4.7}$$

is also treated semi-implicitly.

Ignoring the diffusion terms $K_{\vec{V}_h}$ and K_T which are treated independently in spectral space, the discretized equations read:

Momentum:

$$\begin{aligned}&[\vec{V}_h + \Delta t\, \beta\, \nabla_\eta (\gamma\, (T(t+\Delta t)-T(t)) + R_d T_r (\ln p_s(t+\Delta t)-\ln p_s(t)))]^+ = \\ &[\vec{V}_{hf} - \Delta t\, \beta\, \nabla_\eta (\gamma\, (T(t-\Delta t)-T(t)) + R_d T_r (\ln p_s(t-\Delta t)-\ln p_s(t)))_f]^- \\ &+ 2\, \Delta t\, [\vec{MT}]^0\end{aligned} \tag{4.8}$$

where $\vec{MT}$ is the explicit right hand side of the momentum equation without diffusion.

Applying the operator $\vec{k} \cdot \vec{\nabla}_\eta \times$ to this equation we get:

$$\xi^+ = L \tag{4.9}$$

and with the operator $\vec{\nabla}_\eta \cdot$

$$[D + \Delta t\ \beta\ \nabla^2(\gamma\ T + R_d\ T_r\ \ln p_s)]^+ = M \tag{4.10}$$

In order to calculate the r.h.s. of these equations, one has to add together vectors referring to different points and therefore they have to be expressed in a common reference frame. This reference frame has been chosen to be the unit vectors lying on the tangential plane at the middle of the trajectory.

The discretized thermodynamic equation is

$$[T + \Delta t\ \beta\ \tau\ D]^+ = T_1 \tag{4.11}$$

and the continuity equation

$$(\ln p_s + \Delta t\ \beta\ \nu\ D)^+ = l_0 \tag{4.12}$$

Eliminating $(\ln p_s)^+$ and T^+ we finally get

$$(1 - \Gamma\ \nabla^2)\ D^+ = DT' \tag{4.13}$$

where the matrix Γ is a constant coefficient matrix with dimension the number of vertical levels. This equation is easily solved in spectral space as the spherical harmonics are eigenvectors of the laplacian operator.

The diagnostic equations for computing $\dot{\eta}$ and ω as well as the hydrostatic equation are integrated in the vertical using the same scheme as in the previous operational model.

5. AVERAGING OF EXPLICIT TERMS ALONG THE TRAJECTORY

The right-hand side terms in the equations include some values with a 0 superindex. This means evaluation of such terms at the present time and at the middle of the trajectory. Such an evaluation can be performed by interpolation to this point using the surrounding points or by means of averaging between their values at both ends of the trajectory (using values at the present time). The averaging is written in general as

$$\tilde{F}_0(t) = \frac{\alpha}{2}\ (F_+(t) + F_-(t)) + (1 - \alpha)F_0(t) \tag{5.1}$$

Currently $\alpha=1$ for the momentum equations

$\alpha=0$ for the thermodynamic and continuity equations.

6. TRAJECTORY CALCULATION

The usual iterative procedure to calculate the middle of an upstream trajectory in semi-Lagrangian models is:

$$r^{n+1} = g - \Delta t\, \dot{r}^{n} \tag{6.1}$$

where g is the position of the arrival grid point, r is the middle of the trajectory, $\dot{r}$ the velocity at r and the superindex indicates the iteration number.

The procedure is graphically sketched in Fig. 4. As a first guess to the trajectory of the parcel arriving at point G, we take the three-dimensional velocity V^0 and track back during one time-step to point r^0. The velocity V^1 is found by means of 3-dimensional linear interpolation to point r^0 and, tracking back with this velocity from the arrival point G, a new centre of the trajectory is found as point r^1. The procedure can be iterated more times but in the present operational version only this first iteration is made as further iterations have shown negligible efect on the cases tested.

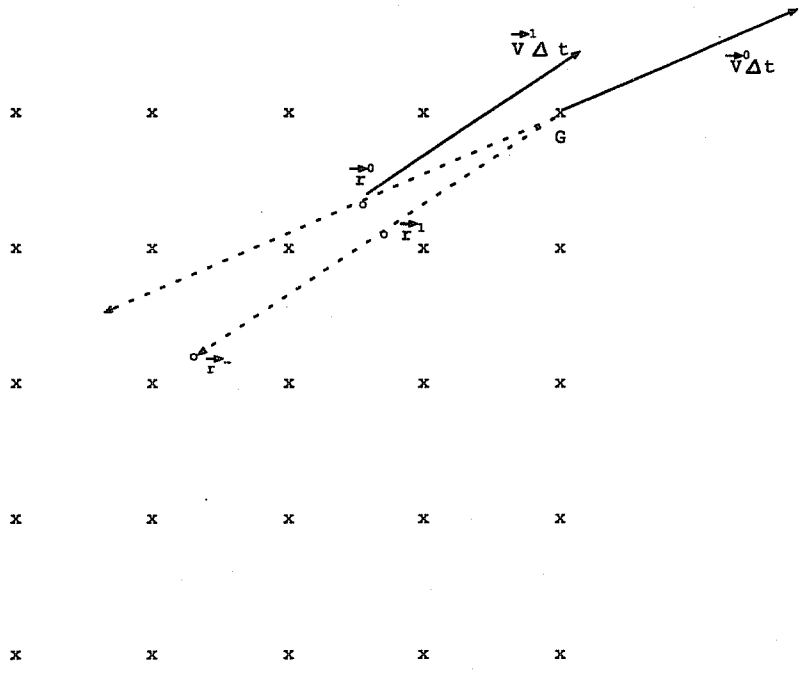

Fig. 4 Iterative trajectory calculation in two dimensions over a regular grid. V^0 is the first guess velocity for the trajectory going back from point G during two time steps. $\vec{r} = G - 2\,\Delta t\, V^1$.

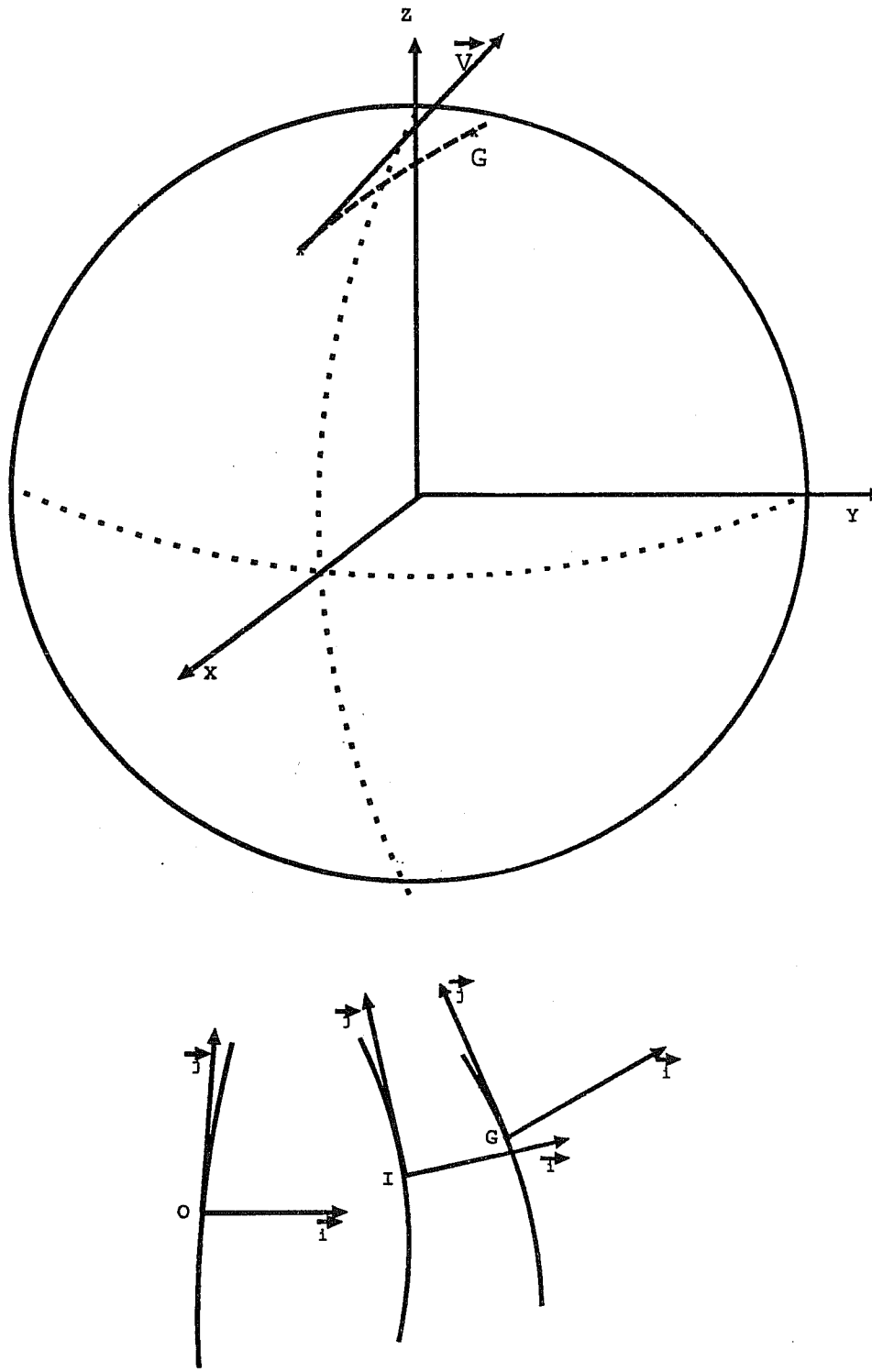

Fig. 5(a) Trajectory calculation over the sphere as a great circle using the auxiliary cartesian coordinate system centered at the centre of the Earth.
(b) The reference frames for vector quantities at the end (G), the middle (I) and the start (O) of a trajectory

In Fig. 4 the trajectory is drawn as a straight line. In fact, and particularly near the poles the latitude circles are too curved, therefore the trajectory can not be computed as a straight line in lat-lon coordinates. Instead, it is assumed to be a great circle and it is computed using an auxiliary Cartesian coordinate system centered at the centre of the Earth as shown in Fig. 5(a) where the velocity V refers to the center of the trajectory arriving at point G.

The vector components belonging to the beginning, the centre or the end of a trajectory refer to unit vectors which can be quite different and a transformation has to be done to get them on a common reference frame in order to add them together. This common reference system has been chosen to be the tangential plane to the Earth at the centre of the trajectory as in *Ritchie* (1987). This is illustrated in Fig. 5(b). Point G is the arrival point of the trajectory (where we want the new values computed), the horizontal vector quantities of the r.h.s. of the equations related to point O (the departure point) are projected to the reference frame centered at point I (the center of the trajectory) where the computation is made. Then the result is projected to the reference frame of point G.

7. NON ITERATIVE TRAJECTORY CALCULATION AWAY FROM THE POLES

The usual iterative procedure to calculate the middle of an upstream trajectory in semi-Lagrangian models is:

$$r^{n+1} = g - \Delta t\, \dot{r}^{n} \tag{7.1}$$

Assume the speed $\dot{r}$ to vary linearly between grid points in one dimension

$$\dot{r} = a + b\, r \tag{7.2}$$

where $b = \partial \dot{r}/\partial r$, substituting (7.2) in (7.1) we get

$$r^{n+1} = g - a\, \Delta t - b\, \Delta t\, r^{n} \tag{7.3}$$

In order for this procedure to converge, it should have a solution of the form $r = \lambda^{n} + K$ with $|\lambda| \leq 1$.

Substituting in (7.3) we obtain

$$K + \lambda^{n+1} = g - a\, \Delta t - b\, \Delta t\, \lambda^{n} - b\, \Delta t\, K \tag{7.4}$$

therefore

$$K = g - a\, \Delta t - b\, \Delta t\, K \Rightarrow K = \frac{g - a\, \Delta t}{1 + b\, \Delta t} \tag{7.5}$$

and

$$\lambda = -b\,\Delta t \tag{7.6}$$

The procedure is therefore convergent if $|b\,\Delta t| \leq 1 \rightarrow |b| \leq 1/\Delta t$.

Using $\Delta t = 1800\ s \rightarrow 1/\Delta t = 5.10^{-4} s^{-1}$ the procedure should be convergent as the maximum value found for both the horizontal divergence and the derivative of the η vertical velocity with respect to η is $\approx 1.5 \cdot 10^{-5}\ s^{-1}$. This result agrees with the one found by *Pudykiewicz* (1985) in a different way.

Now, the procedure converges towards the value of K given by (7.5) and therefore it should be more accurate to apply this formula instead of (7.1).

The procedure was tested in the framework of the new operational model and found to work well. Nevertheless, formula (7.5) needs the values of the derivatives of the winds as well as the winds themselves at the middle of the trajectory and this interpolation is quite expensive in terms of computing requirements when using the transformed Cartesian coordinates to calculate the trajectory.

The procedure can be applied away from the poles if we make the approximation that the trajectory is a straight line in the spherical lat-lon coordinates but it is not known at present how large an error this approximation entails, nor how far away from the poles it can be applied. Therefore, its implementation inside the model is pending further investigation.

8. REDUCED GAUSSIAN GRID

Resolution is uniform over the sphere when triangular truncation is used for the global spectral representation of atmospheric variables. However much of the computation is performed usually on a Gaussian grid which is regular in longitude and almost regular in latitude, and which is thus far from uniform in its resolution over the sphere. For T213 resolution the longitudinal grid length is only 461 m at the Gaussian latitude closest to the pole while it is 63 km near the equator. Based on the argument that, if a certain grid-length is sufficient at the equator for use in the transform method with triangular truncation, then because of the isotropy of this truncation the same grid-length should in practice be sufficient elsewhere, even if a precise alias-free calculation of quadratic terms is not achieved, *Hortal & Simmons* (1991) introduced a reduced Gaussian grid as follows:

The reduced Gaussian grid is the minimal grid for which the longitudinal grid-length does not exceed the grid-length at the equatormost Gaussian latitude and such that the number of points at each row allows the

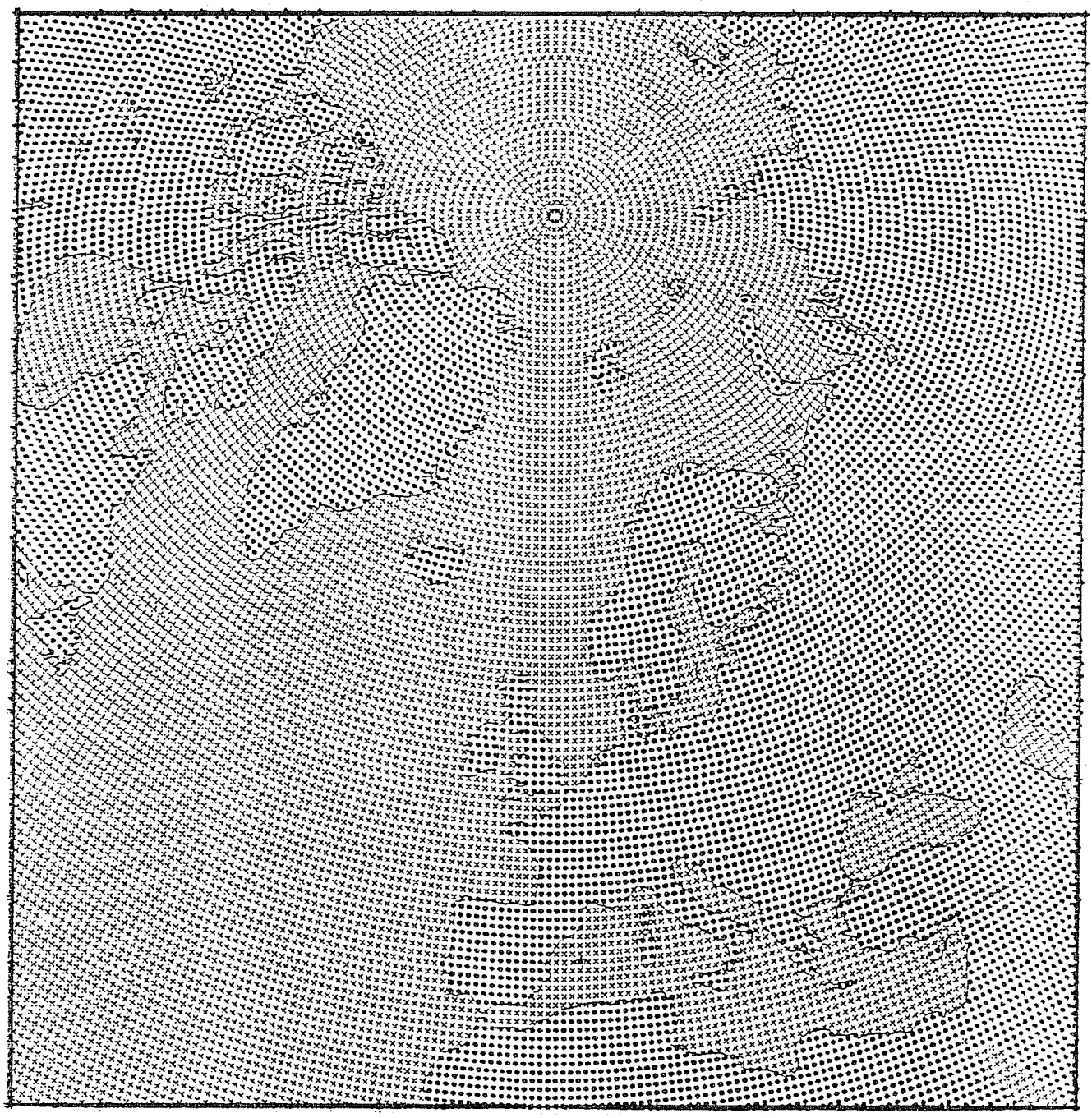

Fig. 6 The T213 Reduced Gaussian Grid. The crosses are considered sea points and the dots land points in the model.

use of the Fast Fourier Transform (FFT) which currently at ECMWF is based on powers of 2, 3 and 5. This gives a much more uniform size for grid-boxes, but there can be a variable staggering of boxes from one latitude line to the next. There are 34.9% fewer points in the reduced grid than in the usual full Gaussian grid at T213 resolution. Correspondingly, the maximum zonal wavenumber that is output from the inverse Legendre transform and input to the direct Legendre transform is (NLN-1)/3 at the row with NLN points.

In some tests using this grid, some noise was apparent in the vorticity field over the poles. The problem largely but not completely disappeared if we kept near the pole all the Fourier components calculated in the direct Fourier transforms consistent with the spectral resolution, instead of truncating at (NLN-1)/3.

This was interpreted as an indication that the resolution near the pole had been reduced excessively and therefore the number of points on the three rows nearest to the poles was increased with respect to the one calculated by the procedure described above. Also, it was decided to keep all the Fourier components at each row {(NLN-1)/2 where NLN is the number of points in the row} as input to the Legendre transforms, as long as they did not exceed in number the model truncation: {(NLON-1)/3) where NLON=max(NLN)}.

Tests comparing results between the reduced grid and the full grid show negligible differences in the forecast up to day 10 but the CPU time is some 27% smaller in the former. Fig. 6 shows the operational T213 reduced Gaussian grid over Europe.

9. INTERPOLATION USING THE REDUCED GAUSSIAN GRID

Interpolation to the departure point using the reduced Gaussian grid does not represent a problem as long as the longitudinal interpolation is performed before the latitudinal one. The only difference between the full and the reduced grid is that a different set of weights has to be used in each of the four rows

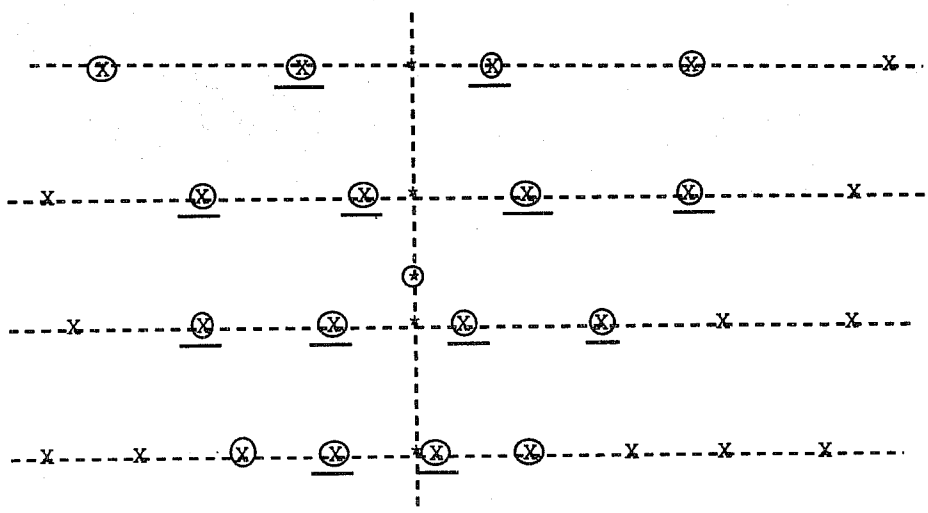

Fig. 7 Points used in the reduced Gaussian grid for different interpolations to the departure point (circled star).

Bi-cubic interpolation is achieved in the horizontal by using the values of the field to be interpolated at the 16 points encircled in Fig. 7. This option was found to be quite expensive in CPU time and therefore, more options were added. The present operational set-up is to use bilinear interpolation, using the four nearest points for the interpolation to the middle of the trajectory both for the velocities in the process of the trajectory calculation and for the explicit terms evaluated at the center of the trajectory, and to use a mixed linear-cubic interpolation for the terms evaluated at the departure point. This mixed linear-cubic interpolation uses linear interpolation at the two farthest rows and cubic interpolation at the nearest rows, therefore using values of the field at the 12 underlined points in Fig. 7.

The same procedure is applied in the vertical interpolation, e.g. the value of the field two levels below or above the departure point is found by bilinear interpolation. When the departure point is above the second highest level or below the second lowest, the vertical interpolation is linear and if the departure point falls above the highest level or below the lowest one, no extrapolation is done, instead the value at the nearest level is used.

There is an option in the model to use non-interpolating semi-Lagrangian treatment of the vertical advection.

In the case of the interpolating scheme, the vertical advection part can be written as:

$$\frac{\partial A}{\partial t} + \dot{\eta}\frac{\partial A}{\partial \eta} = ...$$

which is discretized as:

$$\frac{A^{+} - A^{-}}{\Delta t} = (....)^{0}$$

where A^{-} is the value of the fiels at the origin of the vertical trajectory.

In the non-interpolating scheme, the vertical advection is written as:

$$\frac{\partial A}{\partial t} + \dot{\eta}^{*}\frac{\partial A}{\partial \eta} = ... - \dot{\eta}'\frac{\partial A}{\partial \eta}$$

where $\dot{\eta}^{*}$ is the vertical velocity which would take the parcel to the arrival point from the nearest vertical level to the departure point and $\dot{\eta}'$ is the "residual" vertical velocity $\dot{\eta}' = \dot{\eta} - \dot{\eta}^{*}$.

In this case, the semi-Lagrangian discretization is:

$$\frac{A^+ - A^*}{\Delta t} = (.... - \dot{\eta}' \frac{\partial A}{\partial \eta})^0$$

where A^* is the value of A at the grid point in the vertical nearest to the departure point.

10. SCANNING STRUCTURE

A three scan structure has been implemented in the present version of the model to allow the semi-Lagrangian treatment of the advection terms, a proper parallellization of the code and a more efficient way of calculating the Legendre transforms.

In the first scan the work Fourier files are read row by row from north to south, the east-west derivatives of some fields are computed, the inverse Fourier transforms are applied to go to physical space, the grid-point dynamical non advective calculations are made on the present row and the results kept in a buffer for further use by the semi-Lagrangian scheme and the physics. When a large enough number of rows are present in the buffers to ensure that the air parcels arriving at the central row come from inside the band, the semi-Lagrangian calculations are performed, followed by the physics for this centre row, the direct Fourier transforms are performed, the part of the semi-implicit scheme applied in Fourier space is added and the Fourier coefficients stored in the work file.

In the second scan the Fourier work files are read in wave-number order, the corresponding symmetric and antisymmetric parts computed and the contribution of this wave-number added to the spectral coefficients (direct Legendre transforms). As shown by *Temperton* (1991a), in a U-V formulation, the number of scalar Legendre Transforms needed for time step at each level is 9 (or 8 in a semi-Lagrangian formulation) and these transforms can be computed using only the basic set of Legendre polynomials P_n^m (sin θ). This saves both in the number of transforms performed in a ξ-D model and in the size of the Legendre coefficients file. This number of Legendre transforms does not include the humidity field and therefore a further 3 transforms are needed at each level (at least when the humidity interpolation is not shape-preserving (see Section 13)).

After the second scan, the calculations in spectral space are performed, which include the solution of the Helmholtz equation for the divergence and the addition of the corresponding terms to the thermodynamic and the continuity equations, as well as the diffusion.

In the third scan, the spectral coefficients for U and V are computed from the Divergence and Vorticity, the inverse Legendre transforms applied and the calculation of the Fourier coefficients for every wave-number

computed from their symmetric and anti-symmetric parts and the results stored in the Fourier work file, ready to be used by scan number 1.

11. INITIALIZATION (*Temperton*, 1991)

Implicit normal mode initialization (NMI) was originally developed for use in models for which it is impracticable to compute and use the horizontal normal modes (cf *Temperton*, 1988). Although it requires no explicit knowledge of the modes, it is algebraically equivalent to performing conventional ("explicit") NMI based on the normal modes of a linearized system of equations which is slightly different from the usual choice. For the purposes of initialization, the consequences of this difference in the underlying linear system are negligible except at the largest horizontal scales.

Implicit NMI is also advantageous for high-resolution spectral models, since it avoids the computation and storage of the horizontal modes. In this case, implicit NMI operates directly on the spectral coefficients and reduces to the solution of a few tridiagonal systems for each zonal wavenumber and vertical mode.

As the calculation of the initialization increments is a linear problem in which each zonal wavenumber is treated independently, a scheme can be used in which the first few zonal wavenumbers are treated via the conventional initialization procedure using precomputed normal modes, while the remainder of the spectrum is treated by the implicit procedure. The advantages are twofold: while the size of the "normal mode file" is significantly reduced, the implicit treatment is restricted to the small horizontal scales (where the differences between explicit and implicit NMI are negligible), and the explicit calculation for wavenumbers $m \leq 20$ permits the special handling of the tides and of the filtered diabatic forcing.

At the T213 resolution of the new model, the "normal mode file" is very large, even when restricted to zonal wavenumbers $m \leq 20$. The new initialization scheme takes into account the fact that even for these low zonal wavenumbers, most of the *meridional* modes describe small horizontal scales. Only the large-scale component is treated by the conventional explicit NMI scheme; it includes all the meridional modes required for the handling of the tides and filtered diabatic forcing.

As everything is linear, the two increment vectors for a zonal wavenumber (the large scale one found by the explicit part of the initialization and the short scale one found by the implicit procedure) are added together to produce the initialization increment.

In the present implementation, the meridional cutoff I^0 depends on the zonal wavenumber as

$$I^0 = 39 - m, \qquad 0 \leq m \leq 20.$$

which corresponds approximately to an explicit treatment of initialization for horizontal scales larger than total wavenumber 39.

12. INTERFACE WITH THE PHYSICS

Before adding the semi-implicit contributions to the model equations, we get explicit provisional values of the model variables at the Gaussian grid points. By subtraction of these values from the values at the previous time-step, we get an estimation of the local tendencies, which are then input to the Physics. The Physics package is therefore called once all the explicit dynamical calculations have finished, including the semi-Lagrangian advection calculation.

$$\frac{\partial A_G}{\partial t} \approx \frac{A_G^{e+} - A^-}{2\,\Delta t}$$

Here A_G^{e+} is the provisional new value of field A at grid point G once the explicit dynamical and advection terms have been added.

13. SHAPE-PRESERVING ADVECTION OF HUMIDITY

One of the options included in the model is to perform the interpolation of the humidity field at the upstream location for the semi-Lagrangian advection by means of a shape-preserving algorithm (cf *Williamson et al.*, 1989). In this case, no diffusion is applied to this field and there is no need to transform it to spectral space, therefore sparing some of the Fourier and Legendre transforms, provided a way of computing the virtual temperature gradients, used in the calculation of $\nabla\phi$, is used not requiring the humidity gradients.

The Hermite cubic polynomial interpolant chosen is of the general form

$$p_i = P_i(\theta)/Q_i(\theta)$$

where

$$P_i(\theta) = f_{i+1}\,\theta^3 + (r_i f_{i+1} - h_i d_{i+1})\theta^2(1-\theta) + (r_i f_i + h_i d_i)\theta(1-\theta)^2 + f_i(1-\theta)^3$$

and

$$Q_i(\theta) = 1 + (r_i - 3)\theta(1 - \theta)$$

With $r_i = 3$, Q_i becomes unity and we get the Hermite cubic polynomial interpolant for the interval $[x_i, x_{i+1}]$ of length h_i, given the values of the function at the left (f_i) and the right (f_{i+1}) of the interval and the estimated derivatives (d_i and d_{i+1}) at the same points.

These derivatives are estimated by means of a cubic polynomial interpolation over four points and analytically differentiating the polynomial. The estimated derivatives are then limited at each of the points for shape-preservation inside the corresponding interval according to the *necessary condition for monotonicity* C^0 (cf. *Williamson et al.*, 1989).

The interpolation is first performed at each of the four rows and each of the four vertical levels surrounding the departure point in the longitude dimension and then, from those interpolated values, the same formula is applied in the latitude direction and in the vertical direction. A mixed linear-cubic interpolation is performed by substituting the cubic interpolation on the outer rows by a linear interpolation (which is itself shape-preserving).

14. HORIZONTAL DIFFUSION

A horizontal diffusion of the form ∇^6 is used at resolutions T213 and higher for all fields with the same coefficient of 0.7846×10^{24} $m^6 s^{-1}$ which corresponds to an e-folding decay time of 15 min. for the smallest scales.

For NLEV $\geq$ 31, the default values determining the enhanced horizontal diffusion in the stratosphere are NLVSTDI=2, NLVSTD2=9 and ENSTDIF=$\sqrt{2}$; this means that the diffusion coefficients are enhanced from level 9 upwards until level 2 by a factor of $\sqrt{2}$ at each level. Otherwise, the artificial enhancement of horizontal diffusion at upper levels and in cases of strong wind, used to improve stability of the Eulerian advection scheme, is not invoked if the semi-Lagrangian scheme is used.

On top of this diffusion, an extra diffusion of the form ∇^4 is applied to the divergence field at the uppermost 4 levels, which becomes significant when the maximum wind exceeds 120 m s^{-1} at the corresponding level.

15. ACKNOWLEDGEMENTS

The development of the model presented in this paper has been carried out by a team headed by Adrian Simmons. The initial development of the semi-Lagrangian advection scheme was carried out mainly by Hal Ritchie during a consultancy period he spent at ECMWF.

I thank all the members of the team for their advice during the writing of this paper and particularly A. Simmons and C. Temperton who read the initial manuscript and made several suggestions for its improvement.

REFERENCES

Hortal, M., A.J. Simmons, (1991): "Use of reduced Gaussian grids in spectral models" Mon.Wea.Rev., **119**, 1057-1074.

Pudykiewicz, J., R. Benoit, A. Staniforth, (1985): "Preliminary Results from a Partial LRTAP Model Based on an Existing Meteorological Forecast Model". Atmos.Ocean, **23**, 267-303.

Ritchie, H., (1987): "Semi-Lagrangian advection on a Gaussian grid". Mon.Wea.Rev., **115**, 608-619.

Ritchie, H., (1988): "Application of the semi-Lagrangian method to a spectral model of the shallow-water equations". Mon.Wea.Rev., **116**, 1587-1598.

Robert, A., (1982): "A semi-Lagrangian and semi-implicit numerical integration scheme for the primitive meteorological equations". J.Meteor.Soc. Japan, **60**, 319-325.

Simmons, A.J., D.M. Burridge, (1981): "An energy and angular-momentum conserving vertical finite-difference scheme and hybrid vertical coordinates". Mon.Wea.Rev., **109**, 758-766.

Simmons, A.J., R. Strüfing, (1981): "An energy and angular-momentum conserving finite-difference scheme, hybrid coordinates and medium-range weather prediction". ECMWF Tech.Rep. No.28, 68pp.

Temperton, C., (1988): "Implicit normal mode initialization". Mon.Wea.Rev., **116**, 1013,1031.

Temperton, C., (1991): "New partially implicit NMI scheme". ECMWF Research Department Memorandum.

Temperton, C., (1991a): "On Scalar and Vector Transform Methods for Global Spectral Models". Mon.Wea.Rev., **119**, 1303-1307.

Williamson, D.L., P.J. Rasch, (1989): "Two-Dimensional Semi-Lagrangian Transport with Shape-Preserving Interpolation". Mon.Wea.Rev., **117**, 102-129.